Centrum voor Wiskunde en Informatica
Centre for Mathematics and Computer Science

H.E. de Swart, J. Grasman

Effect of stochastic perturbations on a spectral model of the atmospheric circulation

Department of Applied Mathematics Report AM-R8515 November

The Centre for Mathematics and Computer Science is a research institute of the Stichting Mathematisch Centrum, which was founded on February 11, 1946, as a nonprofit institution aiming at the promotion of mathematics, computer science, and their applications. It is sponsored by the Dutch Government through the Netherlands Organization for the Advancement of Pure Research (Z.W.O.).

Effect of Stochastic Perturbations on a Spectral Model of the Atmospheric Circulation [1)]

H.E. de Swart and J. Grasman
Centre for Mathematics and Computer Science
P.O. Box 4079, 1009 AB Amsterdam, The Netherlands

The dynamics of a low order spectral model of the barotropic potential vorticity equation, forced by random perturbations, is studied as a function of the memory and intensity of the noise. The unperturbed deterministic system has three equilibria, and for arbitrary initial conditions trajectories in phase space always tend to one of the two stable equilibria representing preferent circulation patterns of the atmosphere. The noise forces the system to visit alternately the two attraction domains of the stable equilibria. During the transition the system will remain for some time in a neighbourhood of the unstable equilibrium. Characteristic residence times in the attraction domains and in the domain near the unstable equilibrium are calculated by combined analytical and numerical methods. Furthermore the alternation of preferent states is studied with a discrete state Markov process model. It consists of three states, which are related to the equilibria of the low order spectral model. Transition probabilities are derived from the characteristic residence times of the stochasticly forced dynamical system. The eigenvalues of the Markov model yield information about the time scale over which the effect of the initial state is present in the system.

1980 Mathematics Subject Classification: 76C15,60J70,34A50
Key Words & Phrases: stochasticly forced spectral model, Fokker-Planck equation, characteristic residence time, eikonal equation, discrete state Markov process.

1. Introduction

The dynamics of the atmosphere has been extensively studied during the past decades. One of the main reasons for this investigation is the problem of weather forecasting, i.e. given an initial state to predict the flow at successive times. It appears that predicted- and actual flow states always tend to diverge after some time. For example, the characteristic error doubling time for the large scale phenomena ($O(10^6 m)$) in a numerical model is of the order of a few days. The principal causes for this were sought in the inaccurate specification of the initial state and the limitations of the model to incorporate correctly certain physical processes and boundary conditions. However, recently it has been pointed out (cf. Lorenz, 1984) that the atmospheric flow, which possesses many scales of motion, has an intrinsicly finite range of predictability, which cannot be enlarged by improving the observations.

Since it seems not to be possible to predict the actual flow state of the atmosphere with a sufficiently large probability, it becomes worthwhile to distinguish between weather regimes, i.e. clusters of states representing nearly the same flow pattern. Observations indicate that roughly two preferent types of circulation can be recognized, viz. a high index state with strong westerlies and small wave amplitudes, and a low index state with large waves embedded in a weak zonal flow. The frequently observed blockings, which correspond to highly persistent weather conditions, belong to the latter type. In our study we will identify a third preference regime, which is of transitional type. A more refined division are the Grosswetterlagen defined by Baur, see Egger (1981). Within the framework of long term weather forecasts it is important to obtain a better understanding of the dynamics

1. These investigations were supported by the Netherlands Foundations for the Technical Sciences (STW), future Science Branch of the Netherlands Organization for the Advancement of Pure Research (ZWO).

responsible for the vacillation between the various weather regimes.

More information about the nature of atmospheric variability can be obtained from 500 mb geopotential height analyses, see WALLACE & BLACKMON (1983). They found that the geographical distribution of the variance in the geopotential is mainly determined by the low frequency part of atmospheric waves having time scales of ten days and more. Mechanisms contributing to the low frequency variability are partly external, such as diabatic heating and the large scale topography of the earth, but also internal, due to interactions with the higher frequency transient eddies (OPSTEEGH & VERNEKAR 1982, HOSKINS, JAMES & WHITE, 1983). On the other hand the position and stability of the low frequency waves determine the stormtracks and the structure of the transient perturbations, see e.g. FREDERIKSEN (1983a,b). These results suggest that for long term weather predictions a better understanding is required of the interactions between ultralong quasi-stationary waves and large scale transient eddies.

In studies concerning this subject a planetary scale model is considered, in which the effect of the transient eddies is parameterized in some way. There are several propositions to solve this closure problem. One possibility is to use techniques, originating from turbulence theory, to express the eddy characteristics in terms of the resolved part of the flow. For gridpoint models this has been done by WHITE & GREEN (1982) and SHUTTS (1983). An alternative method is to represent the eddy forcing by stochastic terms, see BALGOVIND et.al. (1983), who applied it to a gridpoint model.

In this paper we study a stochasticly forced spectral model of the large scale atmospheric flow. Such a model can be formulated as a dynamical system of the type

$$\frac{dx}{dt} = f_\mu(x)+F(t) \text{ in } \mathbb{R}^N. \tag{1.1}$$

Here the components $x_i (i = 1,2,...,N)$ of x are amplitudes of the N resolved large scale modes, $f_\mu(x)$ is a vectorfield, depending on parameters $\mu = (\mu_1,\mu_2, \ldots ,\mu_m)$, which describes the internal dynamics of the resolved modes, and the components of $F(t)$ are synoptic forcing terms representing the effect of the short scale unresolved modes on the resolved modes and additional processes not incorporated in the model. In the derivation of the spectral model, of which an example can be found in CHARNEY & DEVORE (1979), we have the freedom to choose the flow characteristics (e.g. barotropic or baroclinic), the geometry of the domain (e.g. a beta plane or the sphere) and the truncation number N.

By application of coarse grain methods from nonequilibrium statistical mechanics, LINDENBERG & WEST (1984) have shown that (1.1) is formally a stochastic differential equation with its stochastic character fully due to the uncertainty in the initial values of the unresolved modes. In some way it confirms the earlier intuitive ideas of CHARNEY & DEVORE (1979) and EGGER (1981) to represent the synoptic forcing terms by stochastic terms. EGGER & SCHILLING (1983,1984) have determined the statistical characteristics of the synoptic forcing terms from data and analysed the response of a linearized version of the barotropic potential vorticity equation. They found that a substantial part of the observed long term variability can be explained as a response of the ultralong waves to this forcing.

Recently, BENZI, HANSEN & SUTERA (1984) and MORITZ (1984) have studied the effect of white noise forcing on three component spectral models of the barotropic potential vorticity equation as a function of the zonal forcing. In this paper we will compute the responses as a function of the intensity and memory of the noise. We assume the short scale waves to be in a statistical equilibrium, hence the $F(t)$ are stationary stochastic terms.

In section 2 a three-component spectral model of the barotropic potential vorticity equation is derived. It appears that for realistic parameter values three equilibria exist. The system always tends to one of the two stable equilibria, which both seem to resemble large scale preference states of the atmosphere (CHARNEY & DEVORE, 1979). We will study the response of this model to white noise and coloured noise processes, which are assumed to represent the effect of the synoptic forcing terms. Mathematical aspects of stochastic processes are considered in more detail in section 3. Due to the noise forcing, transitions between the attraction domains will now occur. The characteristic time of

the system in an attraction domain may be a measure for the persistence of a large scale atmospheric preference state. A method to calculate residence times is discussed in section 4 and results are presented in section 5. Following the ideas of Ghil (pers.comm.) to model geophysical systems by discrete models, we consider in section 6 a Markov model of the atmosphere. It consists of three states, viz. a high index-, a low index- and a transitional state. Transition probabilities per unit of time are specified using the results of section 5. We then calculate the time evolution of the probability distribution from the master equations. The eigenvalues of these equations determine the time scale over which the effect of the initial state is present in this distribution.

2. Derivation and analysis of a low order spectral model

Consider a large scale barotropic flow over a slowly varying topography in the midlatitude beta plane. Let it have a characteristic scale height H, a horizontal length scale k^{-1} and time scale σ^{-1}, and let the topography have a characteristic amplitude h_0. If the meridional scale of the flow is assumed to be much smaller than the radius of the earth r_0, the dynamics is fully governed by a potential vorticity equation. It reads in nondimensional form

$$\frac{\partial}{\partial t}\nabla^2\psi + J(\psi,\nabla^2\psi)+\gamma J(\psi,h)+\bar{\beta}\frac{\partial\psi}{\partial x}+\bar{C}\nabla^2(\psi-\psi^*) = 0, \tag{2.1}$$

where t is time, $\psi(x,y)$ the streamfunction, h the position of the lower boundary and ψ^* is a forcing streamfunction. Furthermore

$$\begin{cases} \nabla = (\frac{\partial}{\partial x},\frac{\partial}{\partial y}), \quad J(a,b) = \dfrac{\partial a}{\partial x}\dfrac{\partial b}{\partial y}-\dfrac{\partial a}{\partial y}\dfrac{\partial b}{\partial x}, \\ dx = r_0\cos\phi_0 d\lambda, \quad dy = r_0 d\phi, \end{cases} \tag{2.2}$$

where λ is the longitude, ϕ the latitude and ϕ_0 a central latitude. All quantities have been scaled according to the scheme given above. The nondimensional parameters read

$$\gamma = \frac{f_0 h_0}{\sigma H};\ \bar{\beta} = \frac{\beta_0}{\sigma k};\ \bar{C} = \frac{f_0\delta_E}{2\sigma H}, \tag{2.3}$$

where $f_0 = 2\Omega\sin\phi_0, \beta_0 = (2\Omega/r_0)\cos\phi_0$ with Ω the angular speed of rotation of the earth. Finally δ_E is the depth of the Ekman layer near the boundary. A derivation of this equation can be found in Pedlosky (1979).

We investigate the existence of travelling wave solutions in a rectangular channel with length L and width B. By letting $k = 2\pi/L$, the nondimensional length and width are 2π and πb respectively, where

$$b = \frac{2B}{L}. \tag{2.4}$$

At the boundaries $y = 0$ and $y = \pi b$ the meridional velocity vanishes and no circulation will develop. Thus the boundary conditions to (2.1) read

$$\begin{cases} \psi(x,y,t) = \psi(x+2\pi,y,t), \\ \dfrac{\partial\psi}{\partial x} = 0 \text{ and } \displaystyle\int_0^{2\pi}\frac{\partial\psi}{\partial y}dx = 0 \text{ at } y = 0, y = \pi b. \end{cases} \tag{2.5}$$

A spectral model is developed by expanding ψ,ψ^* and h in orthonormal eigenfunctions $\{\phi_i\}_{i=1}^{\infty}$ of the two-dimensional Laplace operator. These eigenfunctions are defined in the channel and satisfy (2.5). We only retain the first three modes

$$\psi_1\phi_1 = \sqrt{2}\psi_1\cos(\frac{y}{b});\ \psi_2\phi_2 = 2\psi_2\cos(nx)\sin(\frac{y}{b});\ \psi_3\phi_3 = 2\psi_3\sin(nx)\sin(\frac{y}{b}), \tag{2.6}$$

with ψ_1,ψ_2 and ψ_3 the amplitudes and n an integer. The model is further simplified by taking

$$\psi^* = \psi_1^*\phi_1;\ h = \frac{1}{2}\phi_2. \tag{2.7}$$

Next the spectral model equations are developed for the velocity amplitudes $(x_1,x_2,x_3) = (\psi_1,\psi_2,\psi_3)/b$ of the modes. Putting $\sigma = f_0h_0/H$, $n=1$ and introducing a new time $t = (4\sqrt{2}/3\pi)t$, we obtain

$$\begin{cases} \dot{x}_1 = bx_3 - C(x_1 - x_1^*), \\ \dot{x}_2 = -ab(x_1 - \frac{1}{2}\beta)x_3 - Cx_2, \\ \dot{x}_3 = ab(x_1 - \frac{1}{2}\beta)x_2 - \frac{1}{2}ax_1 - Cx_3. \end{cases} \tag{2.8}$$

Here

$$a = \frac{2b}{1+b^2};\ \beta = \frac{3\pi}{4\sqrt{2}}\bar{\beta};\ C = \frac{3\pi}{4\sqrt{2}}\bar{C},\ x_1^* = \frac{Uk}{\sigma} \tag{2.9}$$

with U a velocity scale of the zonal forcing and x_1^* the driving Rossby number of the flow. Since these equations have been analyzed in detail by CHARNEY & DEVORE (1979) and EGGER (1981), we only summarize the results which are essentail for this paper.

First we note that the divergence of the three- dimensional vectorfield is negative, which means that trajectories are bounded and that for $t\to\infty$ the flow tends to a set of limit points of lower dimension. A stationary point $\hat{x}$ satisfies $f_\mu(\hat{x}) = 0$. For this model $\hat{x} = (\hat{x}_1,\hat{x}_2,\hat{x}_3)$ is found from a cubic equation:

$$\hat{x}_1^3 + a_2\hat{x}_1^2 + a_1\hat{x}_1 + a_0 = 0;\ \hat{x}_2 = \hat{x}_2(\hat{x}_1);\ \hat{x}_3 = \hat{x}_3(\hat{x}_1). \tag{2.10}$$

Here a_2,a_1 and a_0 are known functions of the model parameters, and for each $\hat{x}_1$ we obtain a unique $\hat{x}_2$ and $\hat{x}_3$. There may be one- or three real stationary points, which correspond to equilibrium flow patterns of the basic potential vorticity equation. The set of parameter values for which a transition from one-to three equilibrium states occurs, is called the bifurcation set. In this case it is given by

$$q^3 + r^2 = 0;\ q = \frac{1}{3}a_1 - \frac{1}{9}a_2^2;\ r = \frac{1}{6}(a_1a_2 - 3a_0) - \frac{1}{27}a_2^3. \tag{2.11}$$

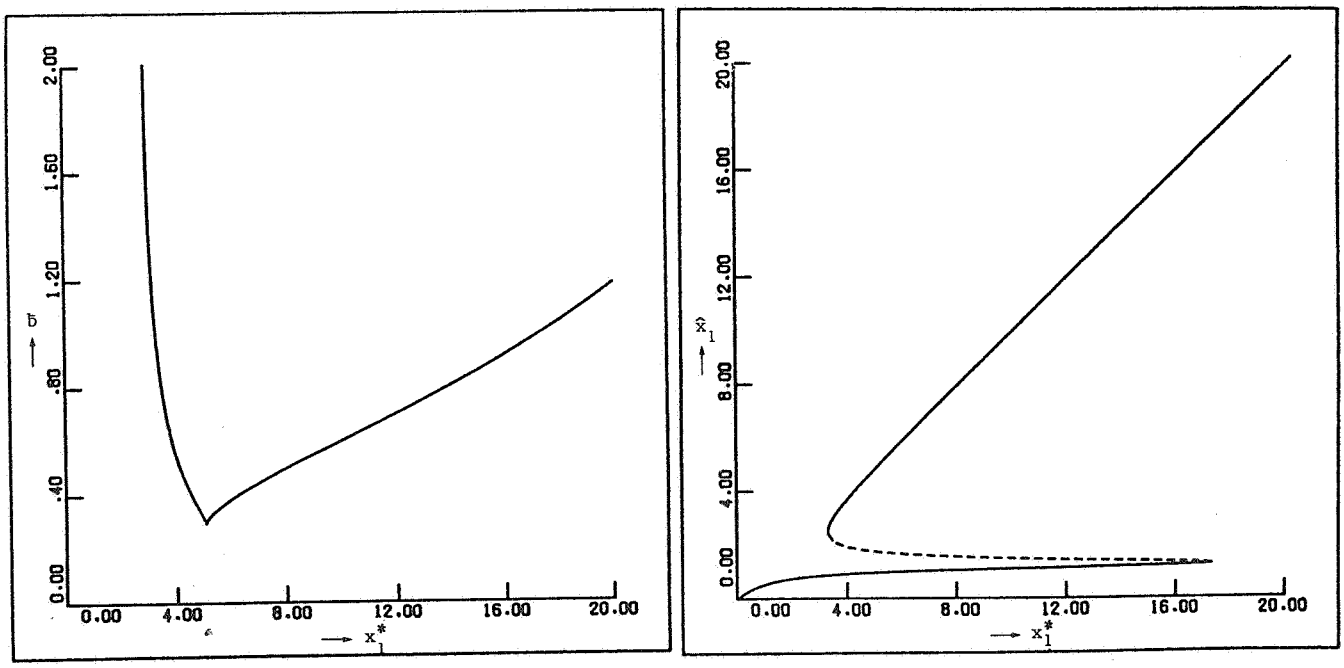

Figure 1 Position of the bifurcation set in the b,x_1^*-parameter space for the atmospheric spectral model described in section 2.

Figure 2 Equilibrium solution $\hat{x}_1$ as a function of x_1^* for $b=1$.

In the region where (q^3+r^2) is negative, called the catastrophe set, three real steady states occur.

We have taken b and x_1^* as free parameters. Furthermore $L = 3.10^6 m$, $h_0 = 500m$, $C = 0.2$ (corresponding to a damping time scale of about fifteen days), $H = 10^4 m$ and at the central latitude $\phi_0 = 45^0$, $f_0 = 1.10^{-4} s^{-1}$ and $\beta = 2.55$. These values are close to those of EGGER (1981). In figure 1 the bifurcation set of the model in the b,x_1^*-parameter space, enclosing the catastrophe set, is shown. In figure 2 the equilibrium solution $\hat{x}_1$ is presented as a function of x_1^* for $b = 1$.

For fixed b and large x_1^* there exists one equilibrium E_1, and a linear stability analysis shows that it is always stable. For decreasing x_1^* two more equilibria appear. The intermediate one (E_2) appears to be unstable, while the lower one (E_3) is stable. For small x_1^* only one equilibrium (E_3) remains. Trajectories in phase space always tend to one of the stable equilibria of the model, except those which (in the case of three equilibria) lie on the separatrix between the attraction domains of E_1 and E_3. Therefore E_2 is of little dynamical significance in this deterministic model. The model behaviour is unrealistic in the sense that the system always ends in an equilibrium state. For a system resembling more closely the atmospheric behaviour we expect frequent transitions between the steady states. This is provided by adding stochastic forcing terms to the equations which will be considered in more detail in the following sections.

3. DYNAMICAL SYSTEMS PERTURBED BY NOISE

In this section we will study a randomly forced dynamical system of the type (1.1). It may be written as a system of stochastic differential equations, i.e.

$$\begin{cases} dx = f_\mu(x)dt + \epsilon \underline{\sigma}(x).d\Phi(t), \\ \Phi(t) = \int_{t_0}^{t} \eta(s)ds. \end{cases} \tag{3.1}$$

For a derivation of these equations see GARDINER (1983). In (3.1) ϵ is a measure of the noise intensity, $\sigma(x)$ is the $(N \times N)$ diffusion matrix and the N components of $\eta(t)$ represent the random forcing. The latter are assumed to be stationary continuous processes, i.e. they are specified by a probability distribution over their range of possible values.

In this way a multivariate stochastic process $X_\epsilon(\eta,t)$ is generated, which takes on the realisations x. In general the evolution at any time will depend on the history of the process, which appears to be fundamental difficulty in the analysis of the dynamics. This problem can be met by choosing the $\eta(t)$ to be white noise processes $\xi(t)$ with the properties

$$<\xi(t)> = 0; \quad \underline{C}(\tau) = <\xi(t)\xi(t+\tau)> = \underline{I}\delta(\tau). \tag{3.2}$$

Here $< >$ denotes an ensemble average over a large number of realisations, and $\underline{C}$ is the correlation matrix. Furthermore I is the $(N \times N)$ unity matrix and $\delta(\tau)$ the Dirac delta function with argument τ. Equation (3.2) shows that white noise processes have zero mean and are fully uncorrelated.

With this choice $\Phi(t)$ becomes a multivariate Wiener process $W(t)$, and the stochastic dynamical system reads

$$dx = f_\mu(x)dt + \epsilon \underline{\sigma}(x) \cdot dW(t). \tag{3.3}$$

Now $X_\epsilon(\xi,t)$ is a Markov process, i.e. its realisation at any time in the future only depends on its present state. Such a process is fully described by the conditional probability density $p(x,t \mid x',t')$, which denotes the probability density for the $X_\epsilon(\xi,t)$ to have the realisation x at time t, given it had realisation x' at time $t' \leqslant t$. It can be shown that $p(x,t \mid x',t')$ is the solution of the Fokker-Planck equation

$$\frac{\partial}{\partial t} p(x,t \mid x',t') = -\nabla \cdot [f_\mu(x) p(x,t \mid x',t')] + \tag{3.4}$$

$$+ \tfrac{1}{2}\epsilon^2 \nabla\nabla : [\underline{\sigma}(x) \cdot \underline{\sigma}^T(x) p(x,t \mid x',t')],$$

where σ^T is the adjungated of σ (GARDINER, 1983). The solution of (3.4) gives a complete description of the stochastic dynamical system (3.3). Another method of obtaining information about the system is the statistical analysis of a large number of simulations of (3.3) by means of a related system of stochastic difference equations, see the appendix.

Representing certain physical processes by white noise can be misleading, because white noise is uncorrelated and its energy is equally distributed over all frequencies in the spectral time domain. Consequently, the noise energy is infinite, and hence the process has no physical relevance. Alternatively we may assume $\eta(t)$ in (3.1) to be coloured noise processes $\zeta(t)$, which are described by the stochastic differential equations

$$d\zeta = -\alpha\zeta dt + \alpha' dW, \tag{3.5}$$

with α and α' nonnegative constants. In order for white noise and coloured noise to result in equal variances of the increments $dx(t)$, we take $\alpha' = \alpha$. We then obtain

$$<\zeta(t)> = 0, \quad \underline{C}(\tau) = \tfrac{1}{2}\alpha e^{-\alpha|\tau|}\underline{I}. \tag{3.6}$$

It follows that α^{-1} is a measure for the correlation time, and the case $\alpha \to \infty$ corresponds to the white noise limit. Some spectral energy distributions of coloured noise for different values of α are shown in figure 3.

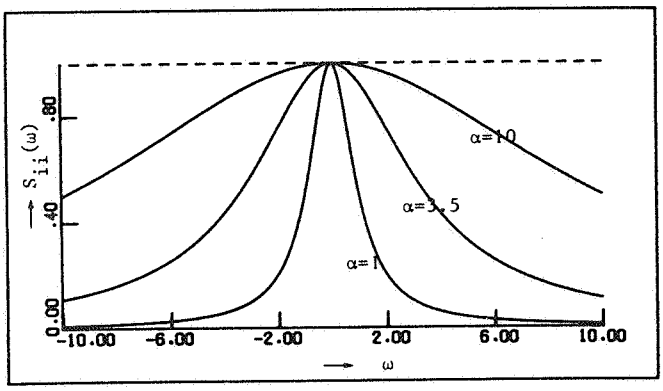

Figure 3 Distribution of energy in the spectral time domain of a coloured noise process for different values of α. The dashed line represents the white noise limit $\alpha \to \infty$.

Applying the coloured noise forcing to (3.1) and transforming $\epsilon\zeta(t) = y(t)$, we obtain the system

$$d\begin{bmatrix} x \\ y \end{bmatrix} = \begin{bmatrix} f_\mu(x) + \underline{\sigma}(x)\cdot y \\ -\alpha y \end{bmatrix} dt + \epsilon \begin{bmatrix} \Theta & \Theta \\ \Theta & \alpha\underline{I} \end{bmatrix} \cdot dW \quad \text{in } \mathbb{R}^{2N}, \tag{3.7}$$

which is of the same type as (3.3). Thus $(X_\epsilon(\zeta,t),\zeta(\xi,t))$ is again a Markov process, and a Fokker-Planck equation for the conditional probability density can be derived from (3.7) in an analogous manner as (3.4) follows from (3.3).

4. ANALYSIS OF THE STOCHASTICLY PERTURBED SYSTEM

We consider the stochasticly perturbed dynamical system (3.3) and assume that the unperturbed system ($\epsilon=0$) has a stable stationary point E. Define in state space a domain $\Omega \subseteq \Omega_a$ containing E, where Ω_a is the attraction domain of E. At the boundary $\partial\Omega$ the deterministic vectorfield satisfies $f_\mu(x)\cdot\nu(x) \leqslant 0$, where $\nu(x)$ is the outward normal to the boundary. Starting in $x \in \Omega$ at time $t=0$, the perturbed system will remain in Ω for a finite time, as shown by MATKOWSKY & SCHUSS (1977). In this section we will derive an expression for the expected residence time $T(x)$ in Ω.

We first analyse the function $\Psi(x)$, satisfying the stationary Fokker-Planck equation

$$L_\epsilon^* \Psi \equiv \tfrac{1}{2}\epsilon^2 \nabla\nabla : [\underline{a}(x)\Psi(x)] - \nabla \cdot [f_\mu(x)\Psi(x)] = 0, \tag{4.1}$$

where

$$\underline{a}(x) = \underline{\sigma}(x) \cdot \underline{\sigma}^T(x), \tag{4.2}$$

see GARDINER (1983). Here the normalisation condition $\Psi(E) = 1$ is proposed.

For low intensity noise ($0 < \epsilon << 1$), an approximate solution is assumed to be of the form

$$\Psi(x) \sim w(x) e^{-Q(x)/\epsilon^2}, \tag{4.3}$$

with $w(E) = 1$ and $Q(E) = 0$. Both $w(x)$ and $Q(x)$ are required to be nonnegative. This WKBJ approximation originates from geometrical optics, see GOLDSTEIN (1980). It is only valid within the attraction domain of E. If Ω coincides with Ω_a, additional boundary layer corrections for $w(x)$ are needed (MATKOWSKY, SCHUSS & TIER, 1983).

Substituting (4.3) in (4.1) and collecting terms with equal power in ϵ, we obtain in lowest order the so-called eikonal equation

$$[\tfrac{1}{2}\underline{a}(x) \cdot \nabla Q(x) + f_\mu(x)] \cdot \nabla Q(x) = 0; \quad Q(E) = 0, \tag{4.4}$$

and in next order the transport equation

$$\begin{cases} [\underline{a}(x) \cdot \nabla Q(x) + f_\mu(x)] \cdot \nabla w(x) + [\nabla \cdot \underline{a}(x) \cdot \nabla Q(x) + \\ + \tfrac{1}{2}\underline{a}(x) : \nabla\nabla Q(x) + \nabla \cdot f_\mu(x)] w(x) = 0; \quad w(E) = 1. \end{cases} \tag{4.5}$$

In our analysis we restrict ourselves to the solution of (4.4). In case a potential function $V_\mu(x)$ exists, such that

$$\begin{cases} f_\mu(x) = f_\mu^{(p)}(x) + f_\mu^{(r)}(x), \\ \underline{a}^{-1}(x) \cdot f_\mu^{(p)}(x) = -\nabla V_\mu(x), \\ \nabla V_\mu(x) \cdot f_\mu^{(r)}(x) = 0, \end{cases} \tag{4.6}$$

then

$$Q(x) = 2\{V_\mu(x) - V_\mu(E)\}. \tag{4.7}$$

When the deterministic system is not of gradient type, a solution is found by writing the left hand side as a Hamiltonian $H(x,p)$, where

$$p = \nabla Q, \tag{4.8}$$

see LUDWIG (1975). The associated Hamilton equations read

$$\begin{cases} \dfrac{dx}{ds} = \underline{a}(x) \cdot p + f_\mu(x), \\ \dfrac{dp}{ds} = -\{\tfrac{1}{2}\nabla \underline{a}(x) \cdot p + \nabla f_\mu(x)\} \cdot p, \end{cases} \tag{4.9}$$

where s is a parameter varying along a bicharacteristic in (x,p) space. Along these bicharacteristics we have

$$\frac{dQ}{ds} = p \cdot \frac{dx}{ds} = \tfrac{1}{2}\underset{\sim}{a}(x) : pp. \tag{4.10}$$

We wish to obtain values for Q at each point $x \in \Omega$, given $Q(E) = 0$. However, from (4.4) and (4.8) it follows that $p = 0$ for $x = E$, which makes it a stationary point of the Hamilton system (4.9). We therefore proceed as follows: near $x = E$ the functions $Q(x)$ and $p(x)$ are approximated by Taylor series:

$$\begin{cases} Q(x) = \frac{1}{2}\underline{P}: (x-E)(x-E)+O(|x-E|^3), \\ p(x) = \underline{P}\cdot(x-E)+O(|x-E|^2), \end{cases} \tag{4.11}$$

where P is a constant matrix. Expanding the vectorfield $f_\mu(x)$ and $a(x)$ near E in Taylor series, substituting the expansions in (4.4) and collecting terms of equal power in $(x-E)$, we obtain in lowest order a matrix Ricatti equation for P, which can be solved by standard methods (LUDWIG, 1975). Thus we have initial values (x_0, p_0, Q_0) for (4.9) and (4.10) on a small sphere around E. Integration of the Hamilton equations yields a path in x-space, called a ray. In this way the solution $Q(x)$ in Ω is constructed.

The expected residence time $T(x)$, defined in the beginning of this section, satisfies Dynkin's equation

$$L_\epsilon T(x) = -1 \text{ in } \Omega; \quad T(x) = 0 \text{ at } \partial\Omega, \tag{4.12}$$

where

$$L_\epsilon \equiv \frac{1}{2}\epsilon^2 \underline{a}(x): \nabla\nabla + f_\mu(x)\cdot\nabla \tag{4.13}$$

is the backward Kolmogorov operator, being the formal adjungated of L_ϵ^* in (4.1), see GARDINER (1983). An approximate solution of (4.12) is found in the low noise intensity limit ($0<\epsilon<<1$) by means of singular perturbation techniques. Using the maximum principle we obtain an asymptotic solution of the form

$$\begin{cases} T \sim C_0 e^{K/\epsilon^2} \text{ outside a neighbourhood of } \partial\Omega, \\ T \sim C_0 e^{K/\epsilon^2}\{1-e^{-\rho/\epsilon^2}\} \text{ near } \partial\Omega \text{ with } f_\mu(x)\cdot\nu(x) < 0, \\ T \sim C_0 e^{K/\epsilon^2} \sqrt{\frac{2}{\pi}} \int_0^{s(x)} e^{-\frac{1}{2}\hat{s}^2} d\hat{s} \text{ near } \partial\Omega \text{ with } f_\mu(x)\cdot\nu(x) = 0, \end{cases} \tag{4.14}$$

and

$$s(x) = \frac{2}{\epsilon}\{\int_0^\rho \tilde{\rho}\frac{\partial f}{\partial \nu}\frac{d\tilde{\rho}}{\underline{a}:\nu\nu}\}^{\frac{1}{2}}.$$

Furthermore ρ is the distance to the nearest point at the boundary and $(\partial/\partial\nu)$ is the derivative along the normal ν. Details can be found in MATKOWSKY, SCHUSS & TIER (1983). The constants C_0 and K can be determined from $\Psi(x)$, following a method developed by MATKOWSKY & SCHUSS (1977). Application of the divergence theorem to the functions $\Psi(x)$ and $T(x)$ yields

$$\int_\Omega \{\Psi L_\epsilon T - T L_\epsilon^* \Psi\} dV = \int_{\partial\Omega} \{\frac{1}{2}\epsilon^2[\Psi\frac{\partial T}{\partial n} - T\frac{\partial \Psi}{\partial n}] - \frac{1}{2}\epsilon^2 \Psi T(\nabla\cdot\underline{a})\cdot\nu + \Psi T f_\mu\cdot\nu\} dS. \tag{4.15}$$

Here $\partial/\partial n = \underline{a}(x):\nu\nabla$ is the conormal derivative. Using (4.3) and (4.12) we obtain

$$-\int_\Omega w e^{-Q/\epsilon^2} dV = \frac{1}{2}\epsilon^2 \int_{\partial\Omega} w e^{-Q/\epsilon^2}\frac{\partial T}{\partial n} dS. \tag{4.16}$$

Both integrals are of Laplace type. Substituting (4.14) in (4.16) we see that the surface integral contains $\exp[-[Q(x)-K]/\epsilon^2\}$. Its main contribution comes from the point $x_{\min} \in \partial\Omega$ where $[Q(x)-K]$ attains a minimum. Since the volume integral is of algebraic order in ϵ, the exponentially large contribution from the surface integral only cancels if

$$K = Q(x_{\min}) = \min_{\partial\Omega} Q(x). \tag{4.17}$$

An integral expression for C_0 can also be found from (4.16). Its analysis requires knowledge of the function $w(x)$, which will not be considered here. In a similar way asymptotic approximations for the distribution of exit points on the boundary $\partial\Omega$ can be derived. As found by MATKOWSKY, SCHUSS & TIER (1983) an ϵ-neighbourhood of $x_{\min}$ is the most probable exit region.

From now on we will assume that Ω coincides with the attraction domain of E and $\partial\Omega$ contains a stationary point $\tilde{E}$ of $f_\mu(x)$. This also applies to the three- component model studied in section 2. From the eikonal equation it then follows $x_{\min} = \tilde{E}$. It implies that unstable equilibria of $f_\mu(x)$ may be of fundamental importance for the dynamics of the stochastic model. As $x \to \tilde{E}$ the deterministic change tends to zero. Consequently, the stochastic system slows down and remains a characteristic time T near that point. Locally, the dynamics is governed by the linearized system

$$\frac{dz}{dt} = \underline{D}\cdot z, \tag{4.18}$$

where D has at least one eigenvalue with positive real part. Starting from an initial point $z_0 = O(\epsilon)$, the eigenvalue with largest positive real part λ_p determines the characteristic time:

$$\tilde{T} = \frac{d}{\lambda_p}\ln(\frac{1}{\epsilon}) + O(1);\ \epsilon \to 0, \tag{4.19}$$

where d is an $O(1)$ constant.

We now discuss in more detail the computation of $K = Q(\tilde{E})$. We introduce in x-space spheres with radius R at the points E and $\tilde{E}$. Next mesh points x_0 are chosen on the sphere at E. The corresponding values of p_0 and Q_0 follow from (4.11). Then equations (4.9)-(4.10) are integrated at each of the mesh points x_0 for the initial values (x_0, p_0, Q_0). If a ray enters the sphere at $\tilde{E}$, the value $Q(\tilde{E})$ is obtained from a Taylor expansion at $\tilde{E}$ similar to (4.11). Next an iteration is carried out: the radius of the spheres is decreased and at each stop a shooting method is applied with the result at the previous step as starting approximation for the angular variables on the sphere at E. The fundamental difficulty in this method is the strong divergence of the rays approaching $\tilde{E}$.

5. RESULTS FOR THE LOW ORDER SPECTRAL MODEL

The theory of sections 3 and 4 will be applied to the three-component spectral model (2.8) with fixed parameter values $b = 1$ and $x_1^* = 4.19$ (corresponding to a channel width of $1{,}5.10^6 m$ and a zonal forcing of $10 ms^{-1}$). Then three equilibria exist:

$$E_1 \sim (3.91, 0.74, -0.06),\ E_2 \sim (1.88, 1.40, -0.46),\ E_3 \sim (0.94, -1.06, -0.65). \tag{5.1}$$

The corresponding streamfunction patterns are shown in figure 4. According to CHARNEY & DEVORE (1979) E_1 and E_3 resemble a zonal- and blocked preference state of the atmosphere respectively. Adding stochastic terms to the equations we obtain a stochastic dynamical system of the type (3.3) or (3.7); we have taken a unity diffusion matrix.

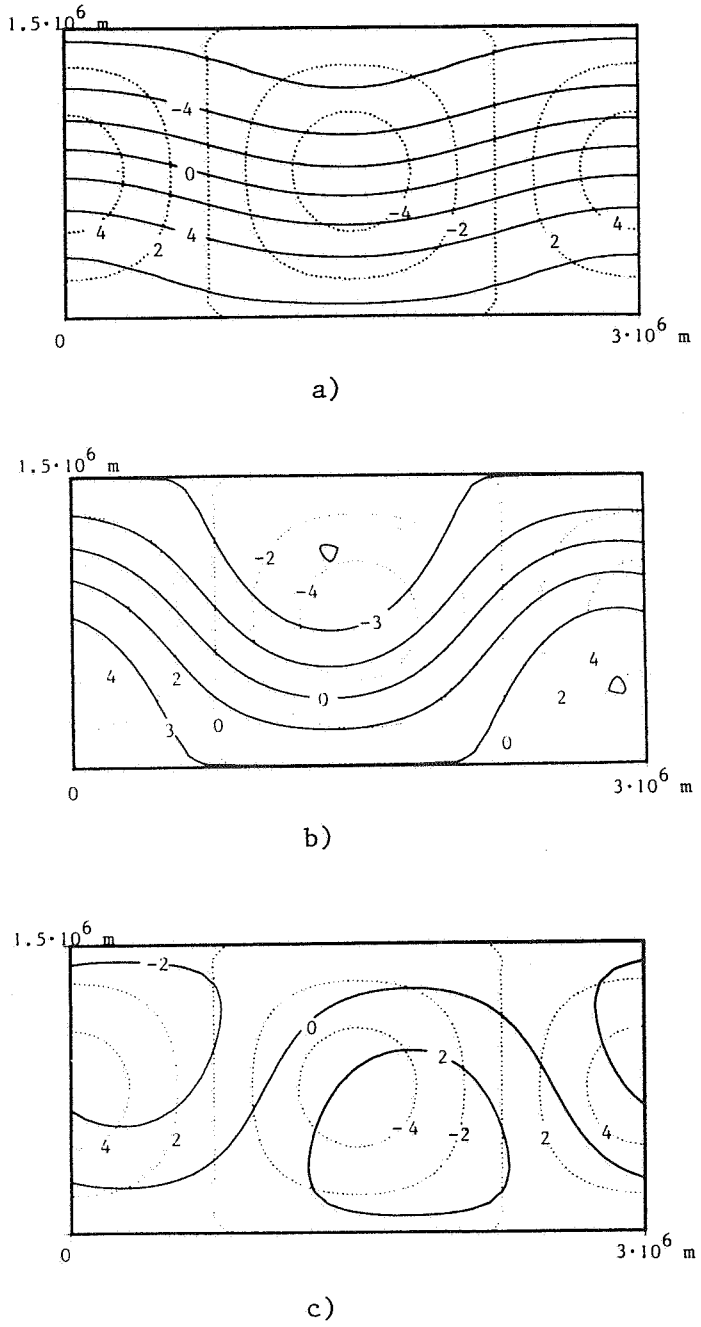

Figure 4 Dimensional streamfunction patterns ($10^6 m^2 s^{-1}$, solid lines) for the equilibrium states $E1(a), E2(b)$ and $E3(c)$ of the atmospheric spectral model described in section 2. The dashed lines represent contours of the orography. The characteristic forcing velocity is 10 ms^{-1}.

We first consider the characteristic residence times near the unstable equilibrium E_2. From a linear stability analysis it was found that $\lambda_p = 0.715$ is the only eigenvalue with positive real part. To verify expression (4.19) a large number (200) of simulations of the system starting in E_2, forced by red noise processes with different values of α, have been carried out. Results are shown in figure 5, where T is plotted against $\ln(1/\epsilon)$ for white noise and a red noise process with $\alpha = 3.5$. The latter value corresponds to a dimensional correlation time of about 1 day, which is representive for the atmospheric flow (EGGER & SCHILLING, 1983). In agreement with (4.19) we find for small ϵ a slope of $1.42 = 1/\lambda_p$, independent of the value of α.

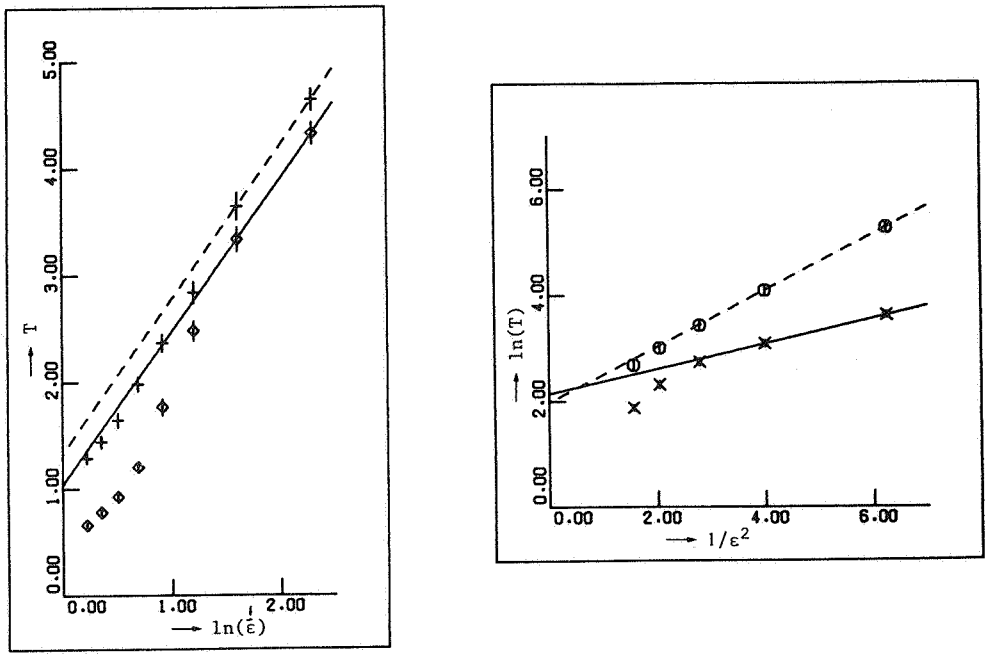

Figure 5 Residence time T near E2 as a function of $\ln(1/\epsilon)$. The solid- and dashed line show the behaviour of T for $\epsilon \to 0$ for white noise and red noise respectively. The data points for white noise forcing are denoted □, and for the red noise +.

Figure 6 ln T (T residence time) in Ω_1 (data points x) and Ω_3 (data points 0) as a function of $1/\epsilon^2$. The solid line and dashed line represent the asymptotic behaviour in the limit $\epsilon \to 0$ for Ω_1 and Ω_3 respectively.

Next we study the residence times in the attraction domains Ω_1 and Ω_3. We distinguish between the white- and coloured noise case. For the first type of stochastic forcing we obtain, by the method of integration along rays, for K in (4.17) the values

$$\begin{cases} K(1) = K(\Omega_1) = 0.23, \\ K(3) = K(\Omega_3) = 0.52. \end{cases} \tag{5.2}$$

Again the results were verified by means of numerical simulations. Figure 6 shows $\ln(T)$ as a function of $1/\epsilon^2$ for the domains Ω_1 and Ω_3. The data are fitted with

$$\ln T = \tilde{K}\frac{1}{\epsilon^2} + \tilde{C}_0, \tag{5.3}$$

The results for $\tilde{K}$ and $\tilde{C}_0$ are

$$\begin{cases} \tilde{K}(1) = 0.24, \quad \tilde{C}_0(1) = 8.5, \\ \tilde{K}(3) = 0.53, \quad \tilde{C}_0(3) = 7.0, \end{cases} \tag{5.4}$$

within an accuracy in $\tilde{K}$ and $\tilde{C}_0$ of 10% and 25% respectively. The K-values agree well with the values in (5.2). Furthermore it appears that the numerical constant C_0 in (4.14) has a significant influence on the expected residence time.

In the case of coloured noise forcing the Hamilton system (4.9) is twelve-dimensional. A shooting method failed, because the bicharacteristics had a strongly diverging character at some distance of E_2. The results for the constants K and C_0 as a function of the noise memory, presented in table 1, are based on numerical simulations only. We remark at this point that in section 2 we have chosen the noise parameterizations in such a way that they result in equal variances of the increments $\Delta x(t)$, where x are the state variables.

It appears that for $0<\epsilon<<1$ the residence times of the system in the two attraction domains increase with increasing noise memory. This can be explained as follows: the time evolution of a system, perturbed by coloured noise, will have some memory of its own. Consequently, larger correlation times cause the system to be persistently driven further away from equilibrium in an arbitrary direction. In the limit $\epsilon \to 0$ it is known that exit through the boundary of an attraction domain will only occur near the unstable equilibrium E_2. Since there is no preference for the perturbation to drive the system right away to this point, it will take a longer time on the average to reach the boundary.

The results shown are based on the assumption that the noise has a low intensity ($0<\epsilon<<1$). We obtained a reasonable agreement between the asymptotic values for the expected residence times and the outcome from simulations for ϵ^2 smaller than 0.3. Estimates of ϵ for atmospheric models are given by EGGER (1981) and EGGER and SCHILLING (1983). They found $\epsilon^2 \sim 0.2$ for the three-component model considered here. In case of white noise forcing it then follows characteristic residence times of about 90 days for the high index state, 10 days for the intermediate state and about 310 days for the low index state. These values seem to be rather large compared with observational data. They even increase by some 10% if coloured noise forcing is applied with a correlation time of one day ($\alpha = 3.5$). Nevertheless, it is remarked that they are of the same order as the average duration of the two preferent weather regimes occuring in the low order baroclinic model of REINHOLD & PIERREHUMBERT (1982), see table 1a in their paper.

6. A DISCRETE STATE MARKOV MODEL OF THE ATMOSPHERIC CIRCULATION

As soon as a stochasticly forced dynamical system of the type (3.1) is in statistical equilibrium, the expected residence times of the preference states yield information about the expected durances of such states. However, in this way no information is obtained about the time scale over which the transient effect of initial conditions are important. To find this time scale in general requires the solution of the full Fokker-Planck equation, but for small noise intensities it appears that most of the time the system is close to a stationary point of the deterministic equations. This suggests the introduction of a discrete state Markov model, with which we can study the evolution of the probability distribution in time for any initial conditions. For the randomly forced spectral model, studied in the previous section, we can develop such a model with three states, viz. a zonal state (1), a transitional state (2) and a blocking state (3).

Let Q_{ij} denote the transition probability per unit time to go from state i to state j ($i,j = 1,2,3$), let $p_i(t)$ denote the probability to be in state i at time t, and let T_i be the characteristic residence time of this state. The latter is a measure of predictability when i is the initial state. The set of discrete time master equations are

$$\begin{cases} p_1(t+\Delta t) = p_1(t)Q_{11}\Delta t + p_2(t)Q_{21}\Delta t + p_3(t)Q_{31}\Delta t, \\ p_2(t+\Delta t) = p_1(t)Q_{12}\Delta t + p_2(t)Q_{22}\Delta t + p_3(t)Q_{32}\Delta t, \\ p_3(t+\Delta t) = p_1(t)Q_{13}\Delta t + p_2(t)Q_{23}\Delta t + p_3(t)Q_{33}\Delta t, \end{cases} \tag{6.1}$$

with Δt a small but finite time step. Since the sum of the probabilities is equal to one, the model can be reduced to two dynamical equations for e.g. $p_1(t)$ and $p_3(t)$ and one passive equation for $p_2(t)$. To arrive at the time-continuous model we use the identities

$$\sum_{j=1}^{3} Q_{ij}\Delta t = 1 \quad \text{for} \quad i = 1,2,3, \tag{6.2}$$

and take the limit $\Delta t \to 0$. The result is

$$\begin{cases} \dfrac{dp_1}{dt} = -(Q_{12}+Q_{13}+Q_{21})p_1 + (Q_{31}-Q_{21})p_3 + Q_{21}, \\ \dfrac{dp_3}{dt} = (Q_{13}-Q_{23})p_1 - (Q_{31}+Q_{32}+Q_{23})p_3 + Q_{23}, \\ p_2 = 1 - p_1 - p_3. \end{cases} \tag{6.3}$$

To specify the transition probabilities we use the results of section 5. There it was found that for small noise intensities the transition from the zonal state to the blocking state, and vice versa, occurs by way of the transitional state. Furthermore, given the system is in the transitional state, it has equal probability to go to the zonal state or the blocking state. Hence

$$Q_{13} = Q_{31} = 0; \quad Q_{23} = Q_{21} \tag{6.4}$$

must hold. The remaining unknown coefficients Q_{12}, Q_{21} and Q_{32} in the equations (6.3) can be related to the characteristic residence times in the following way. Define $\chi_i(t)$ as the conditional probability for the system to be in state i at time t, given it was in i at $t=0$. Since $\chi_i(t)-\chi_i(t+\Delta t)$ is the probability for exit of state i in the time interval $[t,t+\Delta t]$, it follows $-d\chi_i/dt$ a probability density distribution over the time domain. Consequently the characteristic residence time is

$$T_i = -\int_0^\infty t\frac{d\chi_i}{dt} = \int_0^\infty \chi_i dt, \tag{6.5}$$

where in the last step partial integration has been applied. In this case we have

$$\begin{cases} \chi_1(t)-\chi_1(t+\Delta t) = \chi_1(t)Q_{12}\Delta t, \\ \chi_2(t)-\chi_2(t+\Delta t) = 2\chi_2(t)Q_{21}\Delta t, \\ \chi_3(t)-\chi_3(t+\Delta t) = \chi_3(t)Q_{32}\Delta t. \end{cases} \tag{6.6}$$

Developing for $\Delta t \to 0$ and using (6.5) we finally obtain

$$Q_{12} = \frac{1}{T_1}, \quad Q_{21} = \frac{1}{2T_2}, \quad Q_{32} = \frac{1}{T_3}. \tag{6.7}$$

Our model now consists of (6.3), (6.4) and (6.7). The general solution of this inhomogeneous linear system can be written

$$\begin{bmatrix} p_1 \\ p_3 \end{bmatrix} = \begin{bmatrix} p_{1s} \\ p_{3s} \end{bmatrix} + \alpha_1 \begin{bmatrix} u_{11} \\ u_{13} \end{bmatrix} e^{\lambda_1 t} + \alpha_2 \begin{bmatrix} u_{21} \\ u_{23} \end{bmatrix} e^{\lambda_2 t}, \tag{6.8}$$

where

$$\begin{bmatrix} p_{1s} \\ p_{3s} \end{bmatrix} = \frac{1}{T_1+2T_2+T_3} \begin{bmatrix} T_1 \\ T_3 \end{bmatrix} \tag{6.9}$$

is the equilibrium point of the model, which corresponds to the stationary probability distribution. Furthermore λ_1 and λ_2 are eigenvalues of the homogeneous system with (u_{11},u_{13}) and (u_{21},u_{23}) the eigenvectors; α_1 and α_2 are integration constants determined by the initial conditions. It can be shown that λ_1 and λ_2 are real negative constants, so the stationary point is always stable.

As a specific example we have analysed the model for $T_1 = 9$, $T_2 = 1$ and $T_3 = 31$, which are scaled values of the explicitly calculated residence times of section 5. The eigenvalues in this case are

$$\lambda_1 = -0.070, \quad \lambda_2 = -1.073. \tag{6.10}$$

As can be seen from (6.8) they represent a slow- and fast exponential decay towards the stationary probability distribution. In figure 7a) trajectories of the system in the p_1,p_3 −phase plane are shown with initial values (1,0), (0,0) and (0,1), denoting that at $t = 0$ the system is in state 1, 2 or 3 with probability 1. From the numerical experiments it follows that if the system starts in state 1 or 3, the transient evolution of the probability distribution is mainly determined by λ_1. If state 2 is the initial state the decay in p_2 is in a first instance controlled by $\lambda_2 = O(1/T_2)$ and hereafter by λ_1. Thus the predictability is then lower, as the model will almost certain have undergone a transition either to state 1 or state 3. Whenever this happens the dynamics is from then on controlled by λ_1, as we have seen. This is illustrated in the figures 7b), c) and d), which show the time evolution of the probability distribution, starting in the initial states 1, 2 and 3, respectively. The dotted lines show the stationary probability distribution.

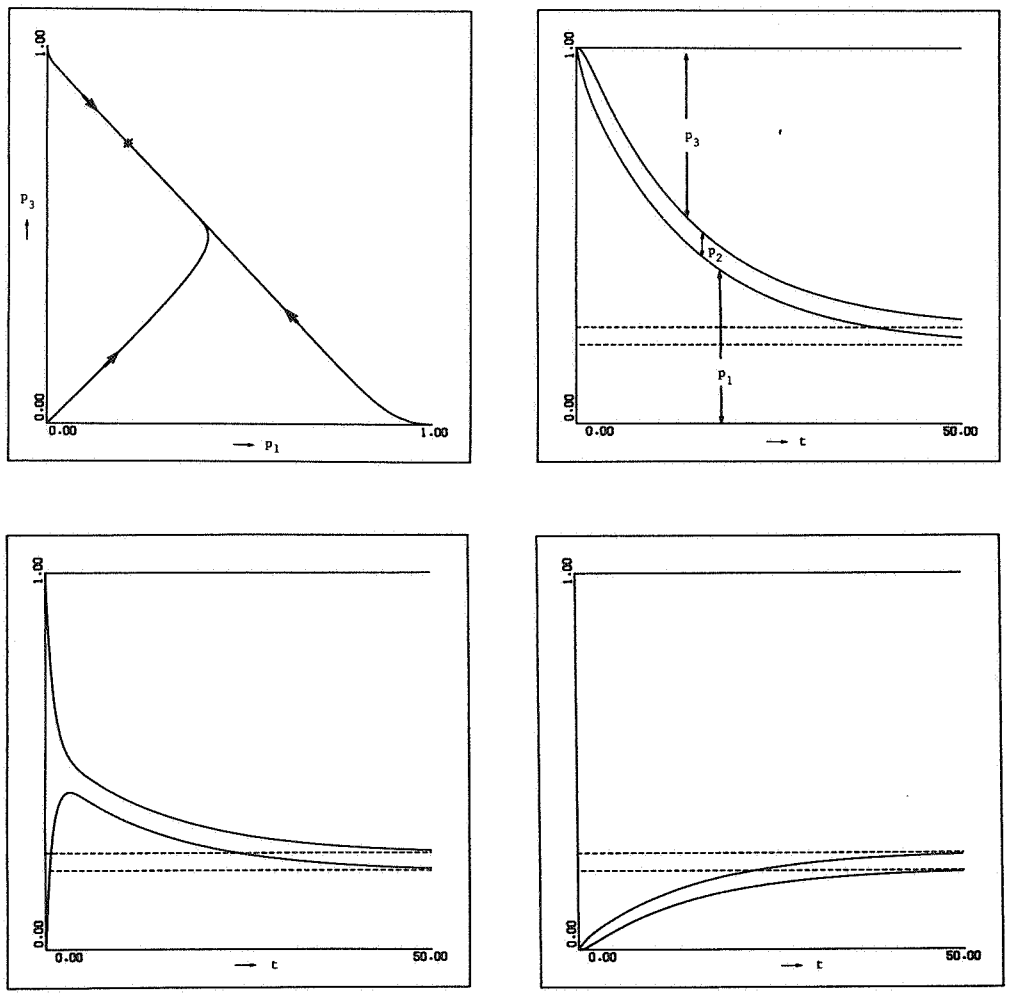

Figure 7 Evolution in time of the probability distribution of the Markov chain model for $T_1 = 9$, $T_2 = 1$ and $T_3 = 31$, starting in the states 1, 2 and 3. In (a) the trajectories in the p_1,p_3- plane are shown. In (*b*)(*c*) and (d) the explicit time dependence is shown; the dotted lines represent the stationary probability distribution.

7. Concluding remarks

In this paper we have studied the effect of stochastic perturbations on a three component spectral model of the barotropic potential vorticity equation on a beta plane. The unperturbed system is considered in section 2. It appeared that for parameter values, representive for the atmosphere, three equilibria E_1,E_2 and E_3 exist. The former and latter are stable, while the intermediate one is unstable.

In section 3 we have parameterised the effect of unresolved modes on the resolved modes, including additional processes not incorporated in the model, by stationary stochastic terms, being of the white noise or coloured noise type. We have taken the diffusion matrix to be the unity matrix. One may include the state dependent sensitivity of the large scale circulation model for transient perturbations by letting the components of the diffusion matrix be functions of the state variables x, but it is not clear how these functions should be specified.

The perturbed system shows frequent transitions between the attraction domains of the stable equilibria E_1 and E_3. As noticed in section 4, for small noise intensities ($0<\epsilon<<1$), the system will also remain for some time in a neighbourhood of the unstable equilibrium E_2, hence the latter is significant for the dynamics of the perturbed system. A method is described to calculate the asymptotic behaviour of the residence times in the neighbourhood of the equilibria for $\epsilon \to 0$. Benzi, Hansen & Sutera (1984) have carried out such an asymptotic analysis. The method we presented extends to unstable equilibria of the unperturbed system and to systems that are not necessarily of gradient type.

In section 5 results were presented for the three component spectral model of atmospheric flow perturbed by noise with different correlation times. It appeared that the shooting method for solving the Hamilton equations was only applicable in the white noise case. For coloured noise forcing results could only be obtained from numerical simulations. The computation of $Q(x)$ by means of integration along rays brings about the difficulty of constructing the ray that connects E with $\tilde{E}$ (see section 4). Presently, we are investigating the possibility of solving a two-point boundary value problem for the Hamilton equations (4.9) with $(x,p)\to(E, 0)$ for $s\to-\infty$ and $(x,p) \to (\tilde{E},0)$ for $s \to \infty$.

Since the solution of the stochasticly perturbed model remains most of the time near the three equilibria of the unperturbed system, we formulated a stochastic dynamical system which may take only three discrete states. In section 6 a time-continuous Markov model is derived to study the transient effects of initial conditions on the evolution of the probability distribution over the three states of the model studied in section 5. From the results it can be concluded that the predictability of the states is closely connected with the eigenvalues of the Markov model. In a first instance the residence times T_i yield information on the expected durance of the preference state i. In addition to this the value $1/\lambda_1$ in (6.10) gives an indication of the time scale over which the effect of the initial state is present in the system. In this time span the initial state can be utilized in the process of computing the probability distribution over the three preference states.

Concerning the validity of the stochasticly forced spectral equations as a model of the atmospheric circulation, it appears that the persistence of the zonal state E_1 and the blocked state E_3 are too large (by a facator of 10) compared to meteorological data. This may be due to the fact that a three component spectral model of the barotropic potential vorticity equation does not include barotropic- and baroclinic instability mechanisms (Charney & DeVore, 1979). The unstable equilibrium E_2 is due to topographic instability, but it seems that in more complicated models this mechanism is of less importance (Hoskins & Revell, 1984). The two stable equilibria E_1 and E_3, representing a zonal- and blocked flow respectively, suggest bimodality in the atmosphere. Although there are some recent indications of the phenomenon, it is not yet confirmed in a systematic data analysis.

Barotropic instability mechanisms can be included in the model by increasing the number of resolved modes. Consequently, the dynamics of the unperturbed system will show a much richer behaviour. From the structure of the spectral model equations it follows that the equilibria of a low order model are also equilibria of higher order models, but their stability properties can be affected by the unresolved modes. For example, a six component spectral model of the barotropic potential

vorticity equation shows in certain domains of the parameter space an unstable equilibrium E_3, with additional equilibria and periodic and aperiodic solutions (CHARNEY & DEVORE, 1979). In a subsequent paper the relation with the stochasticly perturbed three component model will be investigated. A more realistic description of the atmospheric flow is obtained by including vertical resolution in the model. In that case the flow may be baroclinically unstable and show chaotic behaviour (REINHOLD & PIERREHUMBERT, 1982).

APPENDIX

Consider the finite difference scheme of (2.3), which reads

$$x(t+\Delta t) = x(t) + f_\mu(x(t))\Delta t + \epsilon\underline{\sigma}(x(t))\cdot\Delta W(t). \tag{1}$$

For numerical simulations we make the substitution

$$\Delta W(t) \equiv W(t+\Delta t) - W(t) = A(\Delta t)G. \tag{2}$$

Here the components of G are mutually independent Gaussian random generators with zero mean and unit standard deviation, a choice based on the properties of the Wiener process. Furthermore $A(\Delta t)$ is a function of the time step Δt which has to be chosen in such a way that the parameterisation (2) does not affect the variances of the increments $<\Delta x(t)\Delta x(t)>$ in (1), i.e.

$$<\Delta W(t)\Delta W(t)> = A^2(\Delta t)<GG> \tag{3}$$

must hold. Using the property

$$<W(t)W(t+\tau)> = min(t,t+\tau)\underline{I}, \tag{4}$$

we find that the left hand side of expression (3) equals $\Delta t\underline{I}$. For the chosen random generators $<GG> = \underline{I}$, and thus from (3)

$$A(\Delta t) = \sqrt{\Delta t}. \tag{5}$$

Hence the numerical scheme for equation (2.3) reads

$$x(t+\Delta t) = x(t) + f_\mu(x(t))\Delta t + \epsilon\underline{\sigma}(x(t))\cdot G\sqrt{\Delta t}. \tag{6}$$

Finally we remark that there are two conditions on the time step. First,

$$\Delta t \ll 1, \tag{7}$$

in order to avoid instabilities due to the deterministic integration. Secondly, in the limit $\epsilon \to 0$ we expect the variance of the difference between the stochastic- and deterministic trajectories to be zero. Therefore we must also require

$$\Delta t = o(\epsilon);\ \epsilon \to 0. \tag{8}$$

ACKNOWLEDGEMENT

The authors are grateful to Dr. J.D. Opsteegh, of the Royal Netherlands Meteorological Institute, for his suggestions on the modelling of the large scale atmospheric circulation and for his critical reading of the manuscript.

REFERENCES

BALGOVIND, R., A. DALCHER, M. GHIL and E. KALNAY (1983), *A stochastic-dynamic model for the spatial structure of forecast error statistics,* Mo.Wea.Rev. **111,** 701-722.

BENZI, R., A.R. HANSEN and A. SUTERA (1984), *On stochastic perturbation of simple blocking models,* Quart. J.R. Met.Soc. **110,** 393-409.

CHARNEY, J.G. and J.G. DEVORE (1979). *Multiple flow equilibria in the atmosphere and blocking,* J. Atm. Sc. **36,** 1205-1216.

EGGER, J. (1981), *Stochastically driven large-scale circulations with multiple equilibria,* J. Atm. Sc. **38,** 2608-2618.

EGGER, J. and H.D. SCHILLING (1983), *On the theory of the long-term variability of the atmosphere,* J. Atm. Sc. **40,** 1073-1085.

EGGER, J. and H.D. SCHILLING (1984), *Stochastic forcing of planetary scale flow,* J. Atm. Sc. **41,** 779-788.

FREDERIKSEN, J.S. (1983a), *A unified three-dimensional instability theory of the onset of blocking and cyclogenesis II: teleconnection patterns,* J. Atm. Sc. **40,** 2593-2609.

FREDERIKSEN, J.S. (1983b), *The onset of blocking and cyclogenesis, linear theory,* Austr. Met. Mag. **31,** 15-26.

GARDINER, C.W. (1983), *Handbook of stochastic methods for physics, chemistry and the natural sciences,* Springer Verlag, 442 pp.

GOLDSTEIN, H. (1980), *Classical mechanics (2th ed.),* Addison-Wesley Pu. Co. Inc., 672 pp.

HOSKINS, B.J., I.N. JAMES and G.H. WHITE (1983), *The shape, propagation and mean-flow interaction of large-scale weather systems,* J. Atm. Sc. **40,** 1595-1605.

LINDENBERG, K. and B.J. WEST (1984), *Fluctuations and dissipation in a barotropic flow field,* J. Atm. Sc. **41,** 3021-3031.

LORENZ, E.N. (1984), *Irregularity, a fundamental property of the atmosphere,* Tellus **36A,** 98-110.

LUDWIG, D., (1975), *Persistence of dynamical systems under random perturbations,* SIAM Rev. **17,** 605-640.

MATKOWSKY, B.J. and Z. SCHUSS (1977), *The exit problem for randomly perturbed dynamical systems,* SIAM J. Appl. Math. **33,** 365-382.

MATKOWSKY, B.J., Z. SCHUSS and C. TIER (1983), *Diffusion across characteristic boundaries with critical points,* SIAM J. Appl. Math. **43,** 673-695.

MORITZ, R.E. (1984), *Predictability and almost intransitivity in a barotropic blocking model,* In: Holloway, G. and B.J. West (eds); *Predictability of fluid motions,* Am. Inst. Phys., 419-439.

OPSTEEGH, J.D. and A.D. VERNEKAR (1982), *A simulation of the January standing wave pattern including the effect of transient eddies,* J. Atm. Sc. **39,** 734-744.

PEDLOSKY, J. (1979), *Geophysical fluid dynamics,,* Springer Verlag, 624 pp.

REINHOLD, B.B. and R.T. PIERREHUMBERT (1982), *Dynamics of weather regimes: quasi-stationary waves and blocking,* Mo. Wea. Rev. **110,** 1105-1145.

REVELL, M.J. and B.J. HOSKINS (1984), *Orographically induced Rossby wave instabilities,* J. Atm. Sc. **41, 51-67.**

SHUTTS, G.J. (1983), *Parameterization of travelling weather systems in a simple model of large-scale atmospheric flow,* Adv. Geoph. **25,** 117-172.

WALLACE, J.M. and M.L. BLACKMON (1983), *Observations of low-frequency atmospheric variability,* In: Hoskins, B.J. and A.P. Pearce (eds); *Large scale dynamical processes in the atmosphere,* Academic Press, 55-94.

WHITE, A.A. and J.S.A. GREEN (1982), *A non-linear atmospheric long wave model incorporating parametrizations of transient baroclinic eddies,* Quart. J.R. Met. Soc. **108,** 55-85.

Table 1

The coefficients $\tilde{C}_0$ and $\tilde{K}$ of (5.3) for different values of α

α	$\tilde{C}_0(1)$ ($\pm 25\%$)	$\tilde{K}(1)$ ($\pm 10\%$)	$\tilde{C}_0(3)$ ($\pm 25\%$)	$\tilde{K}(3)$ ($\pm 10\%$)
1.0	11.0	0.32	11.3	0.68
1.75	10.6	0.30	9.8	0.66
2.5	10.8	0.25	9.3	0.55
3.5	10.2	0.24	8.4	0.53
∞	8.5	0.23	7.2	0.52